α_2-Adrenoceptor-mediated presynaptic inhibition in bulbospinal neurons of rostral ventrolateral medulla

ABDALLAH HAYAR AND PATRICE G. GUYENET
Department of Pharmacology, University of Virginia, Charlottesville, Virginia 22908

Hayar, Abdallah, and Patrice G. Guyenet. α_2-Adrenoceptor-mediated presynaptic inhibition in bulbospinal neurons of rostral ventrolateral medulla. *Am. J. Physiol.* 277 (*Heart Circ. Physiol.* 46): H1069–H1080, 1999.—The rostral ventrolateral medulla (RVLM) controls sympathetic tone via excitatory bulbospinal neurons. It is also the main target of α_2-adrenoceptor (α_2-AR) agonists used for treatment of hypertension. In this study, we examined the synaptic mechanisms by which α_2-AR agonists may inhibit the activity of RVLM bulbospinal neurons. We recorded selectively from RVLM bulbospinal neurons in brain stem slices of neonate rats (P5–P21) using the patch-clamp technique (holding potential −70 mV). α_2-ARs were activated by norepinephrine (NE, 30 μM) in the presence of the α_1-adrenoceptor blocker prazosin. NE induced modest outward currents (5–28 pA) in 70% of the cells that were blocked by barium and by the α_2-AR antagonist 2-methoxyidazoxan. The magnitude of this current was not correlated with the tyrosine hydroxylase immunoreactivity of the neurons. Mono- and oligosynaptic excitatory postsynaptic currents (EPSCs) or monosynaptic inhibitory postsynaptic currents (IPSCs) were evoked by focal electrical stimulation. In all cells, NE decreased the amplitude of the evoked EPSCs in the absence or presence of barium (49 and 70%) and decreased the amplitude of the evoked IPSCs (64 and 59%). The effect of NE on EPSC amplitude was blocked by 2-methoxyidazoxan. Focal stimulation produced a 1- to 2-s EPSC afterdischarge (probably due to activation of interneurons) that was 53% inhibited by NE. In the presence of tetrodotoxin, NE decreased the frequency of miniature EPSCs by 74%. In short, α_2-AR stimulation produces weak postsynaptic responses in RVLM bulbospinal neurons and powerful presynaptic inhibition of both glutamatergic and GABAergic inputs. Thus the inhibition of RVL bulbospinal neurons by α_2-AR agonists in vivo results from a combination of postsynaptic inhibition, disfacilitation, and disinhibition.

presympathetic neurons; C1 cells; norepinephrine; evoked postsynaptic currents; whole cell recordings

DRUGS with α_2-adrenoceptor (α_2-AR) agonist properties such as clonidine are effective for treating moderate to severe forms of hypertension (30). There is general agreement that a major site of action of these drugs is the rostral ventrolateral medulla (RVLM) (31, for review see Refs. 8 and 32), but their precise site of action within this structure remains unknown. The RVLM harbors bulbospinal neurons that send a monosynaptic excitatory projection (presympathetic neurons) to sympathetic preganglionic neurons (6, 27). These neurons are active in vivo and receive convergent excitatory and inhibitory inputs from multiple sources (9). Because some of these cells are inhibited by iontophoretic application of α_2-AR agonists in vivo, postsynaptic inhibition of RVLM presympathetic neurons probably contributes to the sympatholytic action of these substances (1). In support of this interpretation, α_2-AR agonists activate an inwardly rectifying potassium current in many RVLM bulbospinal neurons in vitro (18), and the presympathetic neurons that have a catecholaminergic phenotype (C1 cells) express α_{2A}-ARs as shown by immunocytochemical studies (10). However, postsynaptic inhibition alone seems unlikely to account for the inhibition of RVLM presympathetic neurons caused by systemic administration of clonidine and related drugs. One reason is that only 50% of these cells are noticeably inhibited by iontophoretic application of α_2-AR agonists in vivo (1). Additionally, these agents produce a small potassium current (mean 12 pA) in vitro and only in about two-thirds of the cells (18). Finally, α_2-AR agonists also inhibit calcium currents in the C1 cells of RVLM, which could conceivably lead to an increase in their excitability (20) by decreasing the amplitude of the spike after hyperpolarization as has been reported in caudal raphe neurons (2).

These discrepancies prompted us to test the hypothesis that a presynaptic modulation of transmitter release in RVLM could also contribute to the inhibition of presympathetic neurons and thus contribute to the hypotensive actions of α_2-AR agonists. This hypothesis is supported by the findings that activation of presynaptic α_2-ARs can inhibit glutamate transmission elsewhere in the brain stem, for example, in the spinal trigeminal nucleus (39) and dorsal motor nucleus of the vagus (4).

In the present study, we used a retrograde marker injected into the thoracic spinal cord in combination with the patch-clamp technique to record selectively from identified bulbospinal RVLM neurons in slices. Neurons were recorded exclusively from a narrow region of the medulla from which spinal projections target selectively the spinal laminae involved in autonomic regulation (33, 34). As in our previous work (18), we further characterized whether the recorded neurons could be classified as catecholaminergic C1 neurons using immunostaining for tyrosine hydroxylase. Our aim was to investigate whether norepinephrine (NE) modulates synaptic inputs to these cells. We found that NE activates presynaptic α_2-ARs, leading to a large reduction in excitatory synaptic transmission. Unexpectedly, GABAergic neurotransmission was reduced as well by NE, indicating that α_2-AR activation in the RVLM produces both disfacilitation and disinhibition of bulbospinal RVLM neurons.

Some of these results have appeared in preliminary form (12).

The costs of publication of this article were defrayed in part by the payment of page charges. The article must therefore be hereby marked "*advertisement*" in accordance with 18 U.S.C. Section 1734 solely to indicate this fact.

METHODS

Slice preparation. Sprague-Dawley rat pups (2–3 days old) were anesthetized by hypothermia, and a suspension of fluorescein isothiocyanate (FITC)-tagged microbeads (0.3–0.5 μl; Lumafluor) was injected bilaterally into the upper thoracic spinal cord to retrogradely label presympathetic bulbospinal RVLM neurons. The injection site was not restricted to the intermediolateral cell column because of the small size of the spinal cord. However, RVLM neurons that are retrogradely labeled from the thoracic spinal cord are known to innervate selectively the autonomic cell column (33, 34).

One to eighteen days later, the rats (5–21 days old) were deeply anesthetized by either hypothermia (<7 days old) or halothane (>7 days old). The rats were decapitated, and their brain stems were blocked and immersed in sucrose-artificial cerebrospinal fluid (sucrose-aCSF) equilibrated with 95% O_2-5% CO_2 (pH = 7.38). The sucrose-aCSF had the following composition (in mM): 26 $NaHCO_3$, 1 NaH_2PO_4, 3 KCl, 5 $MgSO_4$, 0.5 $CaCl_2$, 10 glucose, and 248 sucrose.

Coronal slices (200 μm thick) were cut with a Microslicer (Ted Pella, Redding, CA). The optimally located slices were then incubated until used at room temperature (22°C) in lactic acid-aCSF equilibrated with 95% O_2-5% CO_2 (composition in mM: 124 NaCl, 26 $NaHCO_3$, 5 KCl, 1.25 NaH_2PO_4, 2 $MgSO_4$, 2 $CaCl_2$, 10 glucose, and 4.5 lactic acid). For recording, a single slice containing the RVLM was placed in a recording chamber on an upright epifluorescent microscope (Olympus BH-2). The selected slices (one or two per brain) were identified under a ×10 objective by their characteristic pattern of retrograde labeling (18). In this chamber, the slice was continuously superfused at the rate of 1.5 ml/min with normal aCSF equilibrated with 95% O_2-5% CO_2, and all recordings were made at 30–31°C. To prevent precipitation, the aCSF was altered in experiments using barium by eliminating phosphate and sulfate ions (2 mM $MgSO_4$ was replaced with 2 mM $MgCl_2$ and 1.25 mM NaH_2PO_4 was replaced with 1.25 mM NaCl).

Electrophysiological recordings. Neurons containing microbeads were identified under epifluorescence illumination and viewed with a water-immersion ×40 objective using a closed-circuit television camera. We used the "blow and seal" method (35) for the patch-clamp recordings. Positive pressure was continuously applied to the patch pipette, which was advanced under visual control toward neurons in which microbeads were detected. Once the pipette touched the membrane of the selected neuron, the pressure was immediately released and slight negative pressure was applied to establish a high resistance seal. The membrane was then ruptured by further suction to record in the whole cell configuration.

Patch pipettes were pulled from borosilicate glass capillaries with an inner filament (1.5-mm OD, Clark, UK) on a pipette puller (Sutter P87) and were filled with a solution of the following composition (in mM): 114 K-gluconate, 17.5 KCl, 4 NaCl, 4 $MgCl_2$, 10 HEPES, 0.2 EGTA, 3 Mg_2ATP, 0.3 Na_2GTP, and 0.02% Lucifer Yellow (Molecular Probes). Osmolarity was adjusted to 270 mosM and pH to 7.3. The pipette tips were coated with Sylgard, and their resistance was 4–7 MΩ. Whole cell current (fast-clamp mode)- and voltage-clamp recordings were made with an Axopatch-200B amplifier. Liquid junction potential was 9–10 mV, and all reported voltage measurements have been corrected for these potentials. No series resistance compensation was performed.

Electrical stimulation was performed using two tungsten wires, Teflon coated except at their tips (50 μm in diameter, A-M Systems, Everett, WA). They were positioned 100 μm apart and were placed on the surface of the slice 300–400 μm dorsal to the recorded neurons. The stimulation voltage was set at the minimum necessary to induce a maximal evoked postsynaptic current (PSC; potential: 30–50 V, duration: 100–200 μs, frequency: 0.2–0.5 Hz).

Tyrosine hydroxylase immunostaining. After recording was completed, images of the recorded neurons (labeled with Lucifer Yellow) were stored on videotape or digitized using a video card (Snappy video snapshot, Play, Rancho Cordova, CA) and stored in the computer hard disk using JPEG format. This procedure was useful to confirm the identity of the recorded neurons after histological processing, in particular, when recordings were performed from several neurons in the same slice. The slices were fixed in freshly prepared 4% paraformaldehyde in 0.1 M phosphate buffer (pH 7.4). Immunostaining for tyrosine-hydroxylase (TH) was done using an avidin-biotin-based reaction [mouse anti-TH monoclonal antiserum from Chemicon (1:750), biotinylated goat anti-mouse antiserum from Vector (1:150), and streptavidin-conjugated Cy-3 from Jackson (1:1,000)]. The neurons that displayed detectable TH immunoreactivity were considered catecholaminergic. They were assumed to be C1 adrenergic cells, because in double-labeling studies of the RVLM region nearly all bulbospinal TH-immunoreactive cells are also phenylethanolamine *N*-methyl transferase immunoreactive (41). We preferred to use TH rather than phenylethanolamine *N*-methyl transferase immunostaining to identify C1 cells, because our TH antibody provided a more reliable and intense staining than was possible with phenylethanolamine *N*-methyl transferase antibodies available at the time of the study.

Reagents. Drugs and solutions of different ionic content were applied to the slice by switching the perfusion with a three-way electronic valve system. Strychnine HCl, NE bitartrate, *l*-phenylephrine HCl, isoproterenol HCl, prazosin, and 2-methoxyidazoxan (2-MOI) were from Sigma (St. Louis, MO). Endomorphin-1, gabazine (SR-95531), 6-cyano-7-nitroquinoxaline-2,3-dione (CNQX), tetrodotoxin (TTX), desipramine HCl, 5-bromo-*N*-(4,5-dihydro-1H-imidazol-2-yl)-6-quinoxalinamine (UK 14304), and *dl*-baclofen were from Research Biochemicals International (Natick, MA).

Data analysis. During experiments, analog signals were low-pass filtered at 2 kHz (Axopatch 200B), digitized at 48 kHz (Vetter, A. R. Vetter, Rebersburg, PA), and stored on a videotape for later analysis. Off-line, selected recordings of spontaneous PSCs were collected through a Digidata-1200A Interface and digitized at 4–5 kHz using the Fetchex module of pCLAMP6 software (Axon Instruments, Foster City, CA).

For frequency analysis of events in long stretches of data (15–20 min), we used the Fetchan module of pCLAMP6. Event detection was based on the first derivative of the signal after appropriate filtering (100–500 Hz). The threshold criteria (events should exceed an amplitude set between 1.5 and 3 pA/s, for at least 0.5–1 ms in duration) were adjusted to guarantee that no false events would be identified as confirmed by visual inspection for each analysis. These conservative criteria necessitated that a small percentage of probably true events were rejected. The detected events were subsequently grouped and binned (10–70 s) using the Pstat module of pCLAMP6. The presynaptic effects of substances were calculated as changes in the frequency of TTX-resistant PSCs by comparing the baseline frequency of PSCs with the mean frequency of events between the fourth and the sixth minute following the drug application. To determine the drug effect on PSCs evoked by focal electrical stimulation, we averaged 8–20 consecutive evoked synaptic currents 1 min before and 4

min after drug application. For detection of the peak calculation of the amplitude of the evoked PSCs and averaging consecutive evoked PSCs, we used the on-line detection and statistics now available in the Windows version of pCLAMP7 software. The decay time constant of the evoked PSCs was determined by fitting a single exponential from peak to baseline using Origin 4.1 program (Microcal Software, Northampton, MA). Further statistics, plots, and histograms were also performed using Origin 4.1. Data are expressed throughout the text as means ± SE and were analyzed statistically using the paired or unpaired *t*-test unless otherwise stated. In all cases, significance was accepted if $P < 0.05$.

RESULTS

Recordings were made exclusively from RVLM bulbospinal neurons ($n = 63$) identified in the slice by the presence of FITC microbeads in their soma and by their distinctive location in relation to the tip of the inferior olive, the caudal end of the facial motor nucleus, and the base of the medulla (for full anatomic details, see Ref. 18). These neurons were either immunoreactive for TH or intermingled with the lateral group of TH-immunoreactive neurons that project to the spinal cord. Their membrane properties have been studied in detail elsewhere (17, 18) at room temperature. In our conditions (31°C), most of the cells (~70%) were tonically firing at rest (3–4 Hz). The action potentials of 25 randomly selected neurons had an overshoot of 33.1 ± 1.2 mV, an amplitude of 77.3 ± 1.4 mV (range 67–94 mV), and a duration of 2.5 ± 0.1 ms (range 1.6–4.7 ms) calculated at the threshold for spike generation (−44.3 ± 0.7 mV). The input resistance measured between −70 and −80 mV was 619 ± 31 MΩ (range 340–970 MΩ). All neurons were first recorded in current-clamp mode to assess their viability (action potential overshoot > 20 mV), and after a 5-min stabilization period, the neurons were voltage clamped at a potential of −70 mV (holding current of −20 to −80 pA).

Adequate visualization of the neurons was essential to record selectively from bulbospinal RVLM neurons. The patch recordings in this study were made using the "blow and seal" technique (see METHODS) described in detail by Sakmann and Stuart (35). Because of the relatively low density of neurons in the reticular formation and because of the extensive myelinization that occurs in brain stem slices from animals older than 10 days, it was difficult to visualize bulbospinal neurons, which were obscured by the dark myelin sheath that prevented adequate cleaning of the cell surface and the establishment of a tight seal with the patch pipette. However, it was important to verify that our results could be reproduced in at least some neurons taken from mature rats because of possible developmental changes in adrenergic pharmacology. It was also important to compare our results with those obtained using blind intracellular techniques in which NE has been tested on RVLM neurons sampled at random. However, to increase productivity, most of the recorded neurons in this study were made in slices taken from neonatal rat (P_5–P_{12}). Because no qualitative difference was found in the response to α_2-AR activation in neurons taken from older animals (P_{12}–P_{21}; $n = 12$), the results were pooled.

α_2-AR-mediated postsynaptic effect. The postsynaptic response of RVLM bulbospinal neurons to bath-applied substances was evaluated in voltage-clamp recordings at a holding potential of −70 mV (Fig. 1*A*). In the absence of adrenoceptor antagonists, we found that the β-adrenoceptor agonist isoproterenol (10 μM, $n = 6$)

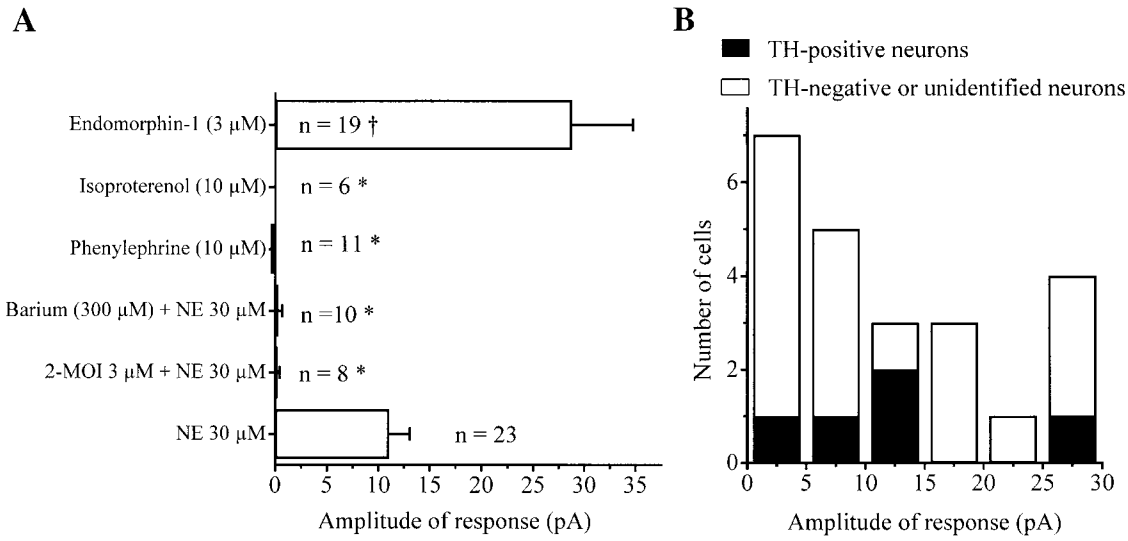

Fig. 1. Postsynaptic effects of norepinephrine (NE) in rostral ventrolateral medulla (RVLM) bulbospinal neurons. *A*: mean amplitude of current produced by NE; comparison with adrenoceptor agonists phenylephrine and isoproterenol and μ-opioid receptor agonist endomorphin-1 (bars indicate means ± SE; *n* = number of neurons tested). Outward current produced by NE was blocked by specific α_2-adrenoceptor (α_2-AR) antagonist 2-methoxyidazoxan (2-MOI) and by barium. *B*: distribution histogram of amplitude of response to NE in all RVLM bulbospinal neurons tested, including the tyrosine-hydroxylase (TH)-immunoreactive neurons. Prazosin (1 μM) was present in the bath in all experiments except those in which phenylephrine was tested. This also applies for all subsequent figures. *Significantly different from NE treatment group (Kruskal-Wallis 1-way analysis of variance on ranks, followed by Dunn's test). †Significantly different from NE treatment group (Mann-Whitney rank sum test).

produced no detectable effect on membrane current, whereas the α_1-adrenoceptor agonist phenylephrine (10 μM, $n = 11$) produced a small inward current (2–3 pA) in only 2 of 11 cells tested. Subsequently, we incubated the slices with the α_1-adrenoceptor blocker prazosin (1 μM) 5–10 min before and during all experiments in which NE was tested.

NE (30 μM, 4 min application) produced a small outward current in 16 of 23 (70%) neurons tested (11 ± 2.1 pA, range 5–28 pA). In the remaining seven neurons, the effect of NE was absent or nondetectable (<5 pA). In three cells that responded to a first application of NE with 10–25 pA, the α_2-AR antagonist 2-MOI (3 μM) blocked the response to a second application of NE (see Fig. 6*A*). Moreover, the first application of NE produced no change in the membrane current in the presence of 2-MOI in five other cells. The magnitude of the outward current produced by NE was compared with that induced by the μ-opiate receptor agonist endomorphin-1 (3 μM, Ref. 44). On average, the amplitude of the outward current produced by endomorphin-1 (29 ± 5.7 pA, $n = 19$) was 2.6 times larger than that produced by NE (Fig. 1*A*). However, the coefficient of variation (SD/mean) of the response to NE and endormorphin-1 was close to 1 because of the large variability in the sensitivity of individual RVLM bulbospinal neurons to either substance.

In several neurons that responded weakly or not at all to NE (<5 pA), application of endomorphin-1 (3 μM, $n = 4$) or the $GABA_B$-receptor agonist baclofen (10 μM, $n = 3$) induced an outward current of 15–55 pA. Thus in these cells the absence of response to NE was not due to the lack of inwardly rectifying potassium channels. We also tested whether the outward current induced by α_2-AR stimulation is sensitive to barium as is the case for $GABA_B$ (18) and μ-opiate receptors in these cells (11). As expected, NE did not produce a detectable outward current in the presence of barium (300 μM, $n = 10$). Moreover, application of barium alone produced a small inward current (2–15 pA), suggesting that a barium-sensitive potassium current is open at rest. Finally, we found that the magnitude of the response to NE was not increased when it was reapplied in the presence of the noradrenergic uptake blocker desipramine (10 μM, $n = 2$), suggesting that α_2-ARs are fully activated at the concentration of 30 μM.

Neurons tested for NE were processed for immunocytochemical detection of the catecholamine-synthesizing enzyme TH. The amplitude of the NE response of TH-immunoreactive neurons was variable with no apparent correlation between the TH immunoreactivity and the α_2-AR agonist sensitivity of the neurons (Fig. 1*B*). This suggests that C1 RVLM bulbospinal neurons could not be distinguished from presumed non-C1 neurons by their postsynaptic sensitivity to NE. Moreover, because NE produced a similar degree of inhibition of synaptic transmission in all RVLM bulbospinal neurons, neurons were not further subdivided according to their chemical phenotype.

Effects of NE on evoked excitatory postsynaptic currents. Excitatory postsynaptic currents (EPSCs) evoked by focal electrical stimulation (~350 μm dorsal to the recording site) were isolated in the presence of the glycine receptor antagonist strychnine (10 μM) and the $GABA_A$-receptor antagonist gabazine (SR-95531, 3 μM, Ref. 25). We used a stimulation intensity that was just sufficient to induce the largest evoked EPSCs. Application of gabazine and strychnine reduced the amplitude of the control evoked postsynaptic current in 14 of 22 cells by a mean of 28 ± 4%, indicating that the release of GABA and glycine mediated a relatively small fraction of the evoked postsynaptic current. In the remaining 6 cells, there was no significant change or a slight increase in the amplitude of the control evoked PSCs (<5%). In 12 of 22 cells, two or more peaks could be distinguished in the evoked EPSCs. In 6 of these 12 neurons, two peaks could still be observed after averaging 8–15 evoked EPSCs, and they were separated by 1.7 to 3 ms (Fig. 2*B*). The first peak was probably monosynaptic because it always occurred with a constant latency after the stimulation artifact. The second peak had a variable latency, suggesting that it involved a disynaptic pathway. The evoked EPSCs had a mean maximal amplitude of 66 ± 7 pA (range 21–127 pA, $n = 22$) and a decay time constant of 5.9 ± 0.3 ms ($n = 22$, range 3.1–8.1 ms) determined by a single exponential fit.

Application of NE (30 μM, 4 min) reversibly reduced the amplitude of the evoked EPSCs in all cells tested by a mean of 49 ± 3% ($n = 9$, range 38–64%). Figure 2*A* shows an example of the effect of NE on an evoked EPSC that exhibited two peaks. As shown in the superimposed traces (Fig. 2*B*), NE did not change the latency of the first peak (presumed monosynaptic current), whereas the second peak was delayed during application of NE. A small rundown in the amplitude of the evoked EPSCs was often observed during the course of such experiments (20–25% reduction after 30 min). Therefore, to compare the effect of repeated applications of NE, the inhibition was calculated relative to a baseline adjusted for the rundown by extrapolation. With the use of this correction factor, the reduction caused by two applications of NE, 15–20 min apart, was the same (first NE challenge 51 ± 6.8% reduction, second NE challenge 47 ± 3.8% reduction, $n = 3$). In another set of experiments, we determined in five cells the effect of the first application of NE in slices treated with 2-MOI (3 μM) for 5–10 min (Fig. 2*B*). In these five cells, NE produced no significant effect on the amplitude of evoked EPSCs (97 ± 2% of control, Fig. 2*C*), indicating that the suppression of the evoked EPSCs by NE was due to α_2-AR activation.

Additional experiments were done in the presence of barium (300 μM) to block inwardly rectifying potassium currents and thus to eliminate any change in conductance due to activation of postsynaptic α_2-ARs. We chose to perfuse the slice with barium instead of recording the neurons with cesium electrodes, because the latter procedure failed to completely block opioid-

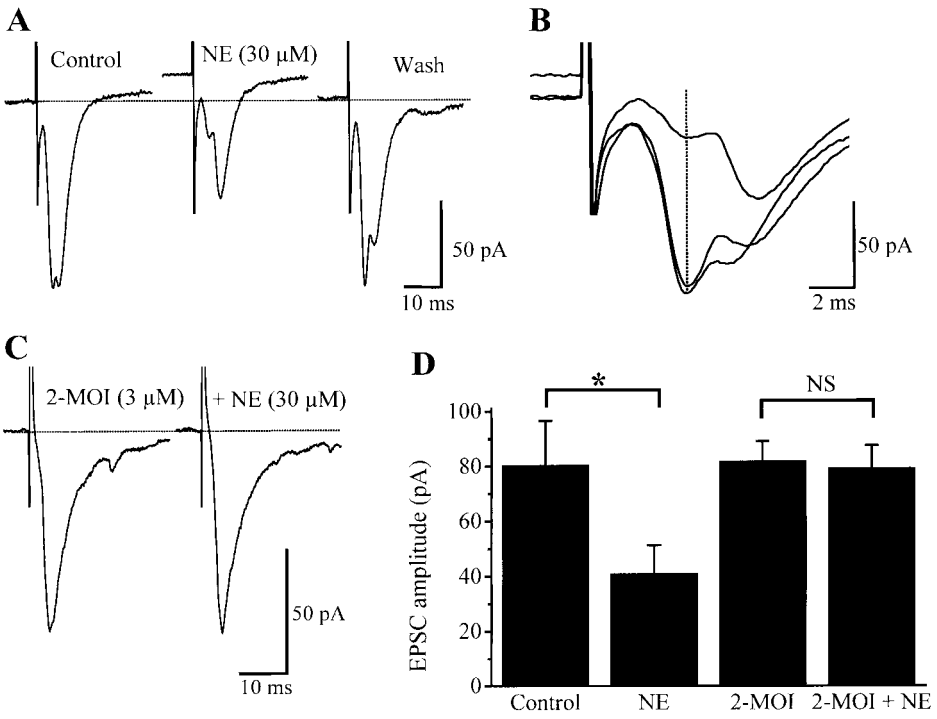

Fig. 2. NE reduces amplitude of evoked excitatory postsynaptic currents (EPSCs) via α_2-ARs. Evoked EPSCs were isolated in presence of gabazine (3 μM) and strychnine (10 μM). Each trace is average of 12–15 consecutive evoked EPSCs [holding potential (HP) = −70 mV]. *A*: NE reversibly decreased amplitude of an evoked EPSC showing 2 peaks. In this neuron (postnatal 10 days), NE induces an outward current shown by upward shift of evoked EPSCs with respect to the baseline holding current (dotted line). *B*: superimposition of 3 traces shown in *A*. Note that latency of first peak was not changed by NE, whereas second peak was delayed. Effects of NE were reversible on washout. *C*: amplitude of evoked EPSC was not changed by NE after application of α_2-AR antagonist 2-MOI (3 μM) in another neuron. *D*: effect of NE on EPSCs amplitude in absence (n = 9) and in presence of 2-MOI (n = 5). *P < 0.001, NS, not significant (P = 0.27).

activated potassium current at negative potentials (43). The reduction in the amplitude of evoked EPSCs by NE persisted in the presence of barium (70 ± 8% reduction with NE, n = 3, Fig. 3). Thus the reduction in excitatory synaptic transmission by α_2-ARs does not involve a barium-sensitive inwardly rectifying potassium current either pre- or postsynaptically.

Effects of NE on evoked inhibitory postsynaptic currents. Inhibitory postsynaptic currents (IPSCs) evoked by focal electrical stimulation were isolated in the presence of CNQX (10 μM). At the holding potential of −70 mV, the IPSCs were recorded as inward currents (Fig. 4), because the calculated equilibrium potential for the chloride ions was −38 mV in our recording conditions. As indicated in the preceding section, the excitatory component of the evoked PSCs predominates because their amplitude was only modestly reduced by antagonists of glycine and GABA receptors. In a previous study, we have shown that the spontaneous IPSCs in RVLM bulbospinal neurons have a relatively longer decay time constant (mean = 19.6 ms) compared with that of spontaneous EPSCs (mean = 4.7 ms, Ref. 12). Therefore, cells in which the evoked PSCs had a decay time constant of >9 ms in control conditions were suspected to receive a significant inhibitory input and were selected for isolating IPSCs. In these cells, application of CNQX reduced the amplitude of the control evoked PSCs by 35 ± 6% (n = 11) and increased their decay time constant by 33 ± 9%. The decrease in the amplitude was probably due to a significant contribution of non-NMDA receptors to the control evoked PSCs. Alternatively, a component of the IPSC could be

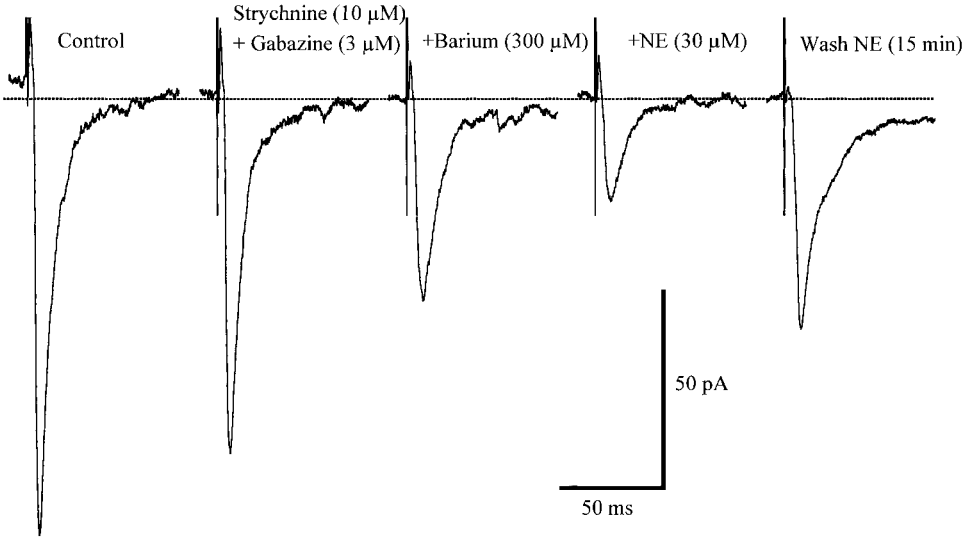

Fig. 3. Presynaptic inhibition by NE in presence of barium (postnatal 6 days, HP = −70 mV). Each trace represents 10 averaged evoked postsynaptic currents (PSCs) obtained from 1 neuron in different conditions. Evoked EPSCs were isolated in presence of gabazine (3 μM) and strychnine (10 μM), which reduced amplitude of control evoked PSCs. Addition of barium (300 μM) further decreased amplitude of evoked EPSCs. Application of NE (30 μM, 4 min) reversibly reduced amplitude of evoked EPSCs without changing holding current (dotted line). Barium was present during application of NE and during its washout.

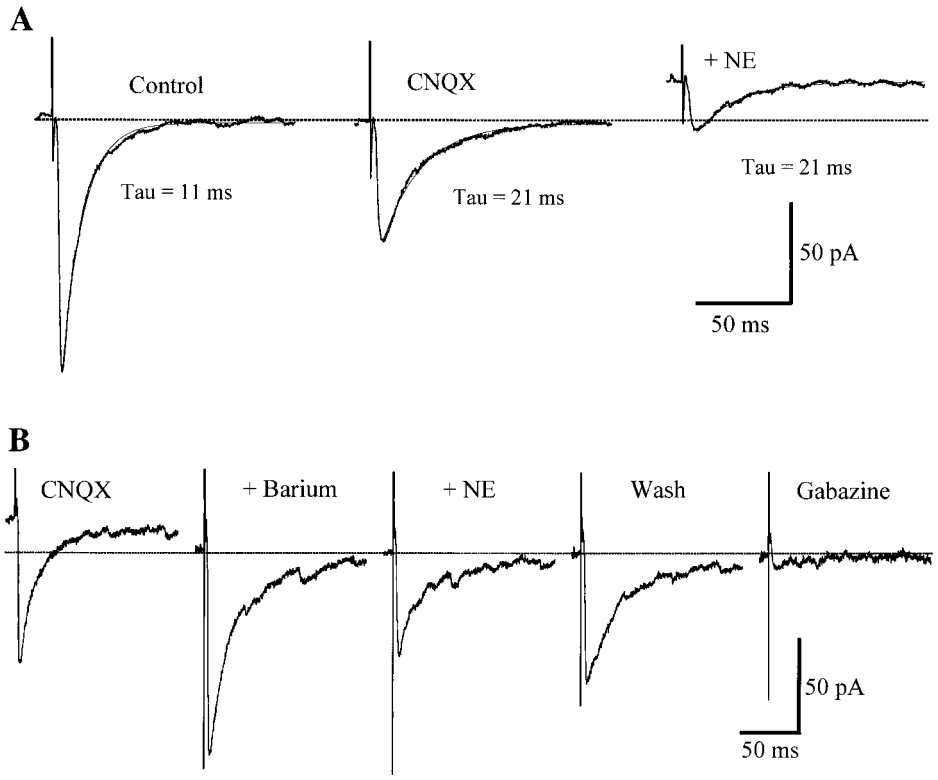

Fig. 4. Reduction of amplitude of evoked inhibitory postsynaptic currents (IPSCs) by NE (30 μM). Evoked IPSCs were isolated in presence of 6-cyano-7-nitroquinoxaline-2,3-dione (CNQX, 10 μM). Each trace is average of 8–12 consecutive PSCs. *A*: perfusion with CNQX decreased amplitude and increased decay time constant of control PSC. Addition of NE decreased amplitude of evoked IPSC without changing its decay time constant. Decay phase of PSC in each trace was fitted with a single exponential (thin curves superimposed on each trace). Note that NE also produced an outward current as indicated by upward shift in baseline of the evoked IPSC (dotted line). *B*: in presence of CNQX, application of barium (300 μM) induced a small inward current and increased amplitude of evoked IPSC. Addition of NE still in presence of barium reversibly decreased amplitude of evoked IPSC without changing holding current (dotted line). Evoked IPSC partially recovered on wash of NE and was blocked by addition of gabazine. Recordings in *A* and *B* are from 2 different neurons (postnatal 7 and 6 days, respectively, HP = −70 mV).

dependent on excitation of inhibitory neurons or terminals. The mean amplitude of the evoked IPSCs was 72.8 ± 15.5 pA (range 29–178 ms), and their decay time constant was 19.3 ± 2.1 ms (range 10.9–39.4 ms), which was about three times longer than that of the evoked EPSCs (see above). Unlike the evoked EPSCs, the evoked IPSCs always consisted of a single peak (Fig. 4), suggesting that they resulted from stimulation of a monosynaptic inhibitory input to RVLM bulbospinal neurons.

NE (30 μM) reduced the amplitude of the evoked IPSCs in all cells tested (n = 9, 3 cells in control medium and 6 cells in presence of 300 μM barium). In the absence of barium, the amplitude of the evoked EPSCs was reduced by 64 ± 7% (n = 3) by application of NE, whereas the decay time constant was not significantly changed (Fig. 4*A*). Barium (300 μM) always increased the frequency of spontaneous IPSCs. The inhibitory effect of NE on the amplitude of the evoked IPSCs persisted in the presence of barium (59 ± 19% reduction, from 74 ± 46 pA in control to 25 ± 11 pA in NE, n = 6; $P < 0.05$), indicating that barium-sensitive potassium channels are not involved in the reduction of IPSCs by NE (Fig. 4*B*). Although barium slightly increased the decay time constant of the evoked IPSCs in some cells, this change was not significant in the six cells tested (from 17.6 ± 3.4 ms in control to 22.3 ± 7.4 ms in barium, P = 0.11). A small increase in the amplitude of IPSC occurred in some cases after barium application (Fig. 4*B*); however, this was not a consistent finding. On average, there was a slight decrease in the amplitude of IPSCs after barium treatment, but this change did not reach statistical significance (from 91 ± 19 pA in control to 74 ± 21 pA in barium, n = 6, P = 0.19). In the presence of barium, NE did not significantly change the decay time constant of the evoked IPSCs (22.3 ± 7.4 ms in control, 20.8 ± 7.8 ms in NE, n = 6, P = 0.44). A small rundown of the amplitude of the evoked IPSCs was also noted during the course of the experiments (see also Ref. 3).

The evoked IPSCs were almost completely abolished (95–100% reduction in amplitude) by additional application of gabazine (3 μM) in six of seven cells tested (Fig. 4*B*). In the remaining cell, the amplitude of the evoked IPSCs was reduced by 70% by gabazine and abolished by further application of strychnine (10 μM). This indicates that GABA rather than glycine made the greatest contribution to the evoked IPSCs in bulbospinal RVLM neurons.

NE effects on spontaneous EPSCs and IPSCs. Spontaneous EPSCs were isolated by incubation with gabazine (3 μM) and strychnine (10 μM). We have previously shown that in RVLM bulbospinal neurons almost all spontaneously occurring PSCs are TTX resistant and have low frequency (12). Rarely (n = 3), we were able to observe spontaneous EPSCs having relatively large amplitude (25–90 pA) and occurring at regular intervals. These EPSCs may be caused by the action potential-dependent release of neurotransmitter from an active interneuron.

The low baseline EPSC frequency (1–3 Hz) could be raised considerably (4–15 Hz) by focal electrical stimulation at low frequency (0.25 Hz, Fig. 5*A*). The EPSCs that were elicited after single electrical stimulation, hence called "EPSC afterdischarge," lasted 1–3 s after each stimulus (Fig. 5*B*). Using this paradigm, we found

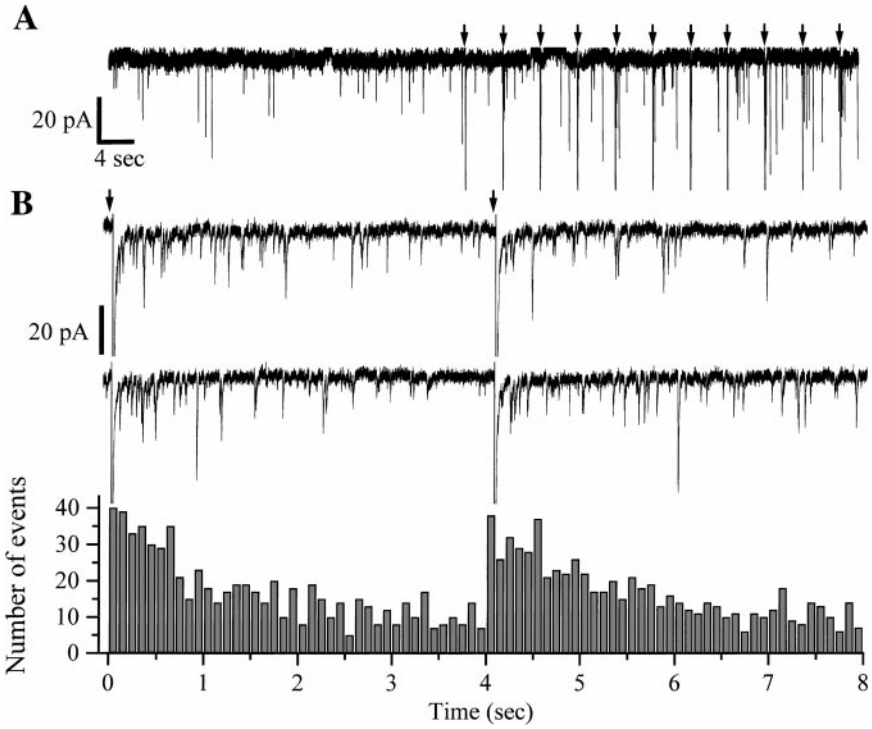

Fig. 5. Long-lasting EPSCs after discharge evoked by focal electrical stimulation. Single electrical stimuli were delivered at 4-s intervals (arrows) in presence of gabazine (3 μM) and strychnine (10 μM). *A*: recording from a neuron showing EPSC activity before and during stimulation paradigm. Note low frequency of events in control (before arrows) and additional EPSCs that appeared and increased in number after many stimuli had been delivered. *B*: traces (*top*) are 2 representative 8-s sweeps in which electrical stimulation (arrows) induced a burst of EPSCs that lasted 1–2 s. Histogram (*bottom*) shows number of events detected (bin = 100 ms) in 15 similar consecutive traces. Note that increase in frequency of spontaneous EPSCs occurred for a period of 2 s after each stimulus. Recordings in *A* and *B* are from 2 different neurons (both postnatal 6 days, HP = −70 mV).

that NE (30 μM) significantly reduced the frequency of EPSCs (6.9 ± 1.9 Hz in control) in all cells tested by an average of 53 ± 3% ($n = 6$, range 43–62%, $P < 0.05$, Fig. 6*A*). NE decreased both the baseline EPSC frequency and the EPSC afterdischarge (Fig. 6*B*). No detectable change in the frequency of EPSCs was observed when NE was applied in the presence of 2-MOI (3 μM, $n = 3$, Fig. 6*A*).

To determine whether the α_2-AR-mediated inhibition of EPSCs occurs at least in part at the level of the synaptic terminals that contact the bulbospinal neurons, we tested the effect of NE on miniature EPSCs (mEPSCs) recorded in the presence of TTX (1 μM) to block action potential-dependent synaptic currents. In five neurons, the frequency of mEPSCs (mean 2.7 ± 0.3 Hz in control) was reduced by 74 ± 3% (range 62–84%, $P < 0.001$) after application of NE (Fig. 7*A*). In three other neurons, the prototypical α_2-AR agonist UK-14304 (10 μM) also reduced the frequency of mEPSCs by 82 ± 6%. In four cells, the reduction of mEPSC

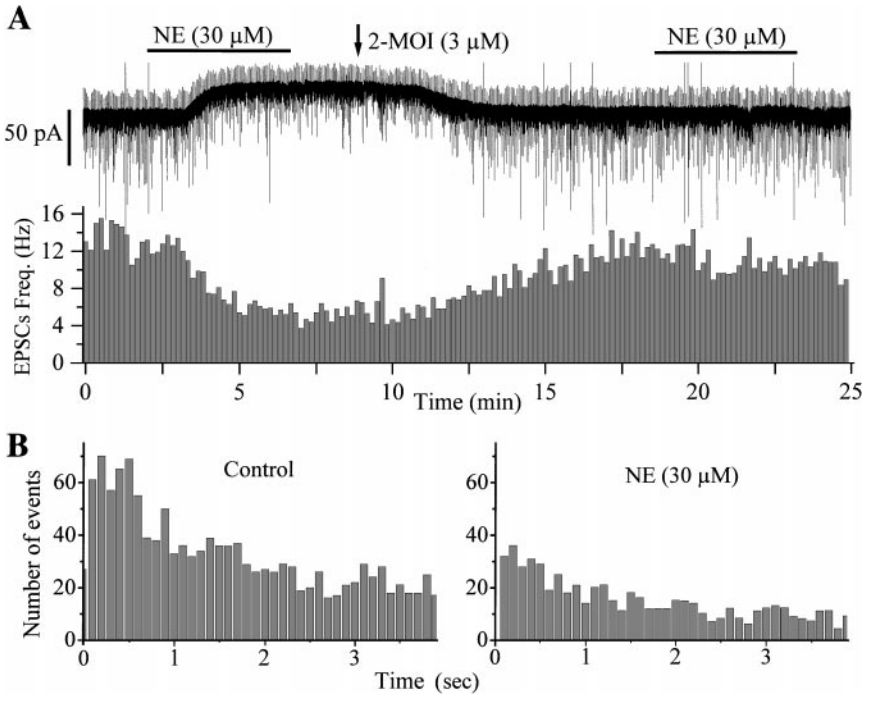

Fig. 6. Effects of NE on spontaneous EPSCs isolated in presence of gabazine (3 μM) and strychnine (10 μM). *A*, *top*: recording from a bulbospinal neuron (postnatal 21 days) in absence of tetrodotoxin (TTX). Electrical stimulation was performed at intervals of 4 s (same protocol as in Fig. 5). Regular upward deflections correspond to stimulation artifacts. Downward deflections represent evoked EPSCs and EPSC afterdischarge. *Bottom*: frequency histogram of EPSCs (bin = 10 s) from same recording. NE induced an outward current and decreased frequency of spontaneous EPSCs. All effects of NE were blocked by perfusion with α_2-AR antagonist 2-MOI. *B*: histograms showing number of EPSCs (bin = 100 ms) detected in 30 consecutive episodes, 4 s each, triggered by electrical stimulation before (*left*) and during (*right*) application of NE. Note that NE decreased frequency of all EPSCs, including those that were induced by electrical stimulation. *A* and *B* are from 2 different neurons (HP = −70 mV).

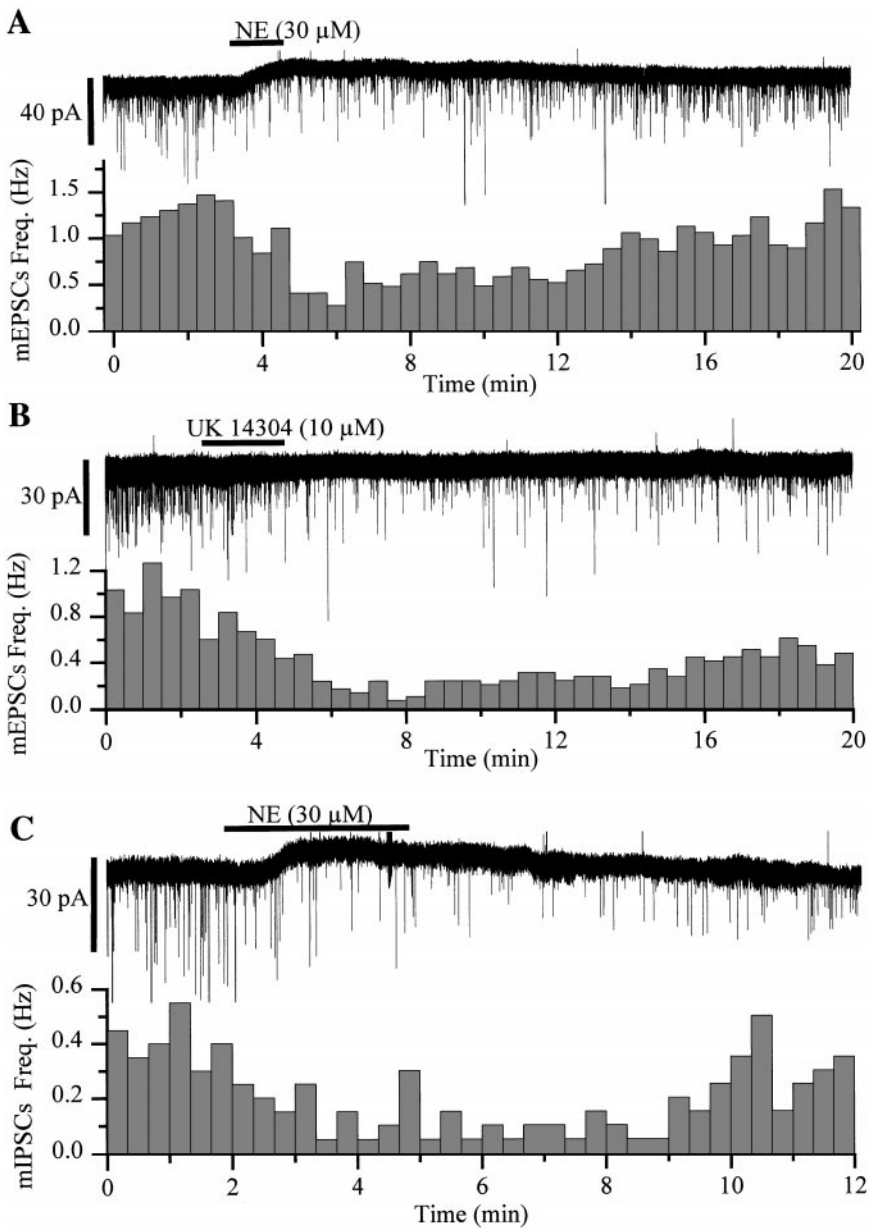

Fig. 7. Decrease of miniature PSC frequency by α_2-AR agonists. Miniature EPSCs (mEPSCs) were isolated in presence of TTX (1 μM), gabazine (3 μM), and strychnine (10 μM), and mIPSCs were isolated in presence of TTX (1 μM) and CNQX (10 μM). Each panel (*A*–*C*) shows a current trace (*top*) and corresponding frequency histogram of mEPSCs (*bottom*). *A*: NE (30 μM) induced a small outward current and a decrease in mEPSC frequency. *B*: in this cell, selective α_2-AR agonist UK-14304 decreased mEPSC frequency without producing an outward current. *C*: NE (30 μM) induced a small outward current and a decrease in mIPSC frequency. Recordings in all panels are from 3 different neurons (postnatal 6–10 days, HP = −70 mV).

frequency by these two α_2-AR agonists occurred even in the absence of detectable outward current (<3 pA, Fig. 7*B*).

We also tested the effect of NE on the frequency of spontaneous IPSCs in nine cells incubated in CNQX (10 μM). In the absence of TTX, NE decreased the frequency of spontaneous IPSCs in all four cells tested by 76 ± 4% (from 3 ± 0.5 Hz to 0.7 ± 0.2 Hz, range 67–95%, $P < 0.05$). In one neuron, NE almost completely eliminated the IPSCs. In this cell, the IPSCs occurred at regular intervals, and they probably reflected the firing of an inhibitory interneuron. In the presence of TTX, the miniature IPSCs were low in frequency (<0.5 Hz), and their frequency was not stable over extended periods of recording. Therefore, it was not possible to determine whether NE could produce any change in the frequency of mIPSCs in three of five cells tested. Nevertheless, a reversible decrease in the frequency of mIPSCs could be reliably observed in the remaining two cells (Fig. 7*C*), suggesting that the reduction in inhibitory synaptic transmission could occur at the level of presynaptic terminals.

DISCUSSION

The major new findings of this study are presented in a hypothetical model (Fig. 8). In brief, NE inhibits bulbospinal RVLM neurons by activating α_2-ARs postsynaptically and α_2-ARs located presynaptically on glutamatergic terminals. Moreover, contrary to our expectations, α_2-ARs are also present on at least some of the GABAergic input to these cells. The decrease of synaptic transmission elicited by NE is not sensitive to barium, indicating that different mechanisms of action are involved in the pre- and postsynaptic effects of NE.

α_2-AR-mediated postsynaptic effects. The mean outward current induced by NE (30 μM) in RVLM bulbospi-

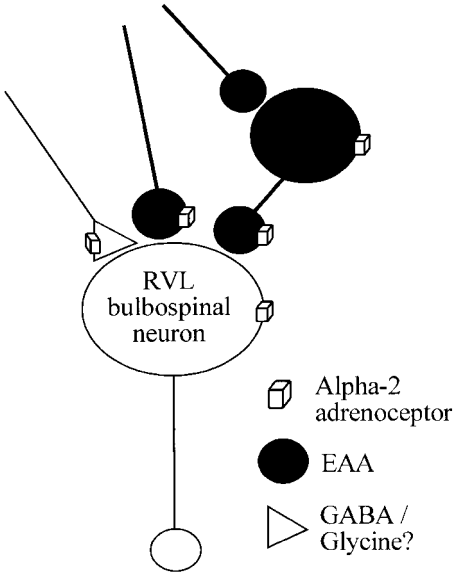

Fig. 8. Presumed location of presynaptic and postsynaptic α_2-ARs in RVLM. About 70% of RVLM bulbospinal neurons have postsynaptic α_2-ARs that are coupled to a potassium conductance. Input to these cells is predominantly excitatory and originates in part from local excitatory interneurons. NE inhibits release of excitatory amino acids (EAA) by activating α_2-ARs located on presynaptic terminals and possibly also on soma of local excitatory neurons. Finally, RVLM bulbospinal neurons receive an inhibitory input that is predominantly GABAergic and subject to inhibition by α_2-AR agonists.

nal neurons was small (11 pA) compared with that caused by the μ-opioid receptor agonist endomorphin-1 (3 μM, 29 pA). This is in agreement with a previous study showing that the α_2-AR agonist α-methylnorepinephrine (30 μM) produced a small and variable outward current (12 pA) in these cells at a holding potential of −50 to −60 mV (18). These results are also consistent with the finding that a large fraction of RVLM bulbospinal neurons recorded in vivo in the adult rat are insensitive to iontophoretic application of α_2-AR agonists (1).

The outward current produced by NE in bulbospinal RVLM neurons was blocked by the selective α_2-AR antagonist 2-MOI (28), confirming that NE produced its effect by activating α_2-ARs (18). In the present study, neither the α_1-adrenoceptor agonist phenylephrine nor the β-adrenoceptor agonist isoproterenol produced a significant effect on membrane current. This is in contrast to previous studies showing that α_1- (13) and β-adrenergic agonists (29, 38) frequently produce excitatory effects in randomly sampled RVLM neurons of adult rats. However, the spinal projection of RVLM is a small percentage of the total neurons (~200 per side in the rat, Ref. 34). Thus it is unlikely that many bulbospinal neurons could be recorded in RVLM by random sampling. Our results suggest that the bulbospinal neurons have an adrenergic pharmacology distinct from that of other RVLM neurons. Alternatively, because most of our neurons were recorded in the neonatal rat, it is possible that α_1- and β-adrenoceptors might be functional only at a later developmental stage.

In a previous study, the outward current produced by α_2-AR activation in RVLM bulbospinal neurons was shown to be inwardly rectifying and to be predominantly carried by potassium ions (18). In the present study, we found that this current is sensitive to barium as is the case for locus coeruleus (5) and A5 noradrenergic neurons (16). It is unlikely that the responses of RVLM neurons to NE were small due to dialysis of intracellular messengers by the pipette solution, because it has been shown that coupling from α_2-ARs to potassium channels is maintained in excised membrane patches (37). In addition, we found that many neurons responded vigorously to activation of $GABA_B$ or μ-opioid receptors after failing to respond to 30 μM NE. It is also unlikely that the absence of effect of NE on the holding current was due to a lack of functional α_2-ARs, because α_2-AR agonists inhibit calcium currents in almost all RVLM bulbospinal neurons (20). In sum, these results indicate that the coupling of α_2-ARs to potassium channels varies between cells possibly because of differential expression of G protein subunits.

The magnitude of the outward current produced by α_2-AR activation was variable in both TH- and non-TH-immunoreactive neurons (Fig. 1). This is in contrast to the A5 region where catecholaminergic neurons were found to be much more uniformly responsive to α_2-AR activation than other noncatecholaminergic neurons (15). Previous in vitro studies have also failed to find consistent differences between the electrophysiological and pharmacological properties of C1 and non-C1 bulbospinal neurons (16–18, 23). Although the magnitude of the current induced by α_2-AR activation is not correlated with the cell phenotype, this current is sufficient, when present, to eliminate the spontaneous discharge of most RVLM bulbospinal neurons in vitro (18).

Properties of EPSCs and IPSCs. Most RVLM bulbospinal neurons have a spontaneous activity in vitro that appears to result from their intrinsic properties (17, 18). Yet, their discharge in vivo is regulated by both excitatory and inhibitory synaptic activity as shown by intracellular recordings (22). Consistent with our previous study on spontaneous PSCs (11), we found that glutamate and GABA are the major contributors to the PSCs evoked by focal electrical stimulation. Indeed, both the spontaneous and evoked PSCs were usually eliminated by a combination of CNQX and gabazine, which block non-NMDA and $GABA_A$ receptors, respectively. The average decay time constant of the evoked IPSCs (19.3 ms) was about three times longer than that of the evoked EPSCs (5.9 ms). These kinetic properties are consistent with our previous study on spontaneous miniature PSCs in which the average decay time constant was found to be 4.7 and 19.6 ms for mEPSCs and mIPSCs, respectively. The kinetic differences between EPSCs and IPSCs probably reflect differences in the properties of non-NMDA and $GABA_A$ channels such as conductance, rate of desensitization, or kinetics of reuptake and degradation of glutamate and GABA.

So far, two main findings suggest that the synaptic input to RVLM bulbospinal neurons is predominantly excitatory. First, antagonists of $GABA_A$ and glycine receptors have only small effects on the amplitude of

evoked PSCs (this study). Second, mEPSCs are usually three to four times more frequent than mIPSCs (11). However, IPSCs may have a strong impact on the excitability of the cells because of their relatively longer decay time constant.

The spontaneous PSCs in RVLM bulbospinal neurons have usually low frequency (<4 Hz), and the vast majority are TTX resistant (11). This suggests that antecedent neurons are either silent at rest or they are active, but their afferent terminals have been severed by the thin-slice procedure. The existence of silent glutamatergic interneurons in RVLM is suggested by two lines of evidence. First, focal electrical stimulation could evoke polysynaptic EPSCs in many RVLM bulbospinal neurons as suggested by the presence of more than one peak in the evoked EPSCs (Fig. 2). Second, in most cases, single electrical stimulation at 0.25 Hz caused a long-lasting EPSC afterdischarge following the evoked EPSCs (Fig. 5). Therefore, under conditions of blockade of fast inhibitory synaptic transmission, electrical stimulation raises the excitability of excitatory interneurons and favors the occurrence of action potential-dependent EPSCs on RVLM neurons.

α_2-AR-mediated presynaptic inhibition. Our results indicate that NE reduces glutamatergic transmission to RVLM bulbospinal neurons in a manner similar to that found in some brain stem neurons (4, 39). NE exerts this inhibitory effect in two ways (Fig. 8). The first mechanism involves a decrease of glutamate release from terminals directly synapsing on RVLM bulbospinal neurons. This is suggested strongly by the decrease in the frequency of TTX-resistant mEPSCs and by the decrease in amplitude of the evoked EPSCs, in particular, the first constant latency peak, which is probably due to a monosynaptic contact. The second mechanism may involve a reduction of the excitability of antecedent presynaptic excitatory interneurons via activation of somatic α_2-ARs. This is supported by the finding that NE decreases the frequency of the presumed action potential-dependent EPSCs that are activated by electrical stimulation (Fig. 6). It is also supported by the finding that NE delays the occurrence of the second, presumably polysynaptic, peak of the evoked EPSCs (Fig. 2). Taken together, these results suggest that NE can exert a powerful inhibitory effect on RVLM bulbospinal neurons by suppressing the activity of the local excitatory network. The suppression of excitatory synaptic transmission by NE is due to α_2-AR activation, because this effect was blocked by the selective α_2-AR antagonist 2-MOI.

Our data also indicate that NE reduces inhibitory synaptic transmission to bulbospinal RVLM neurons via a presynaptic action (Figs. 4 and 7*C*). The IPSCs evoked by focal electrical stimulation in the presence of CNQX were most likely due to monosynaptic stimulation of GABAergic terminals, because they consisted of a fixed latency single peak and they were blocked by additional application of gabazine. To our knowledge, this is the first report of a direct presynaptic modulation of GABAergic transmission by NE in the brain. For instance, in olfactory bulb (40) and the hippocampus (7), NE induces disinhibitory actions indirectly by reducing excitation of inhibitory interneurons.

It is unlikely that the effects of NE on synaptic transmission are due to postsynaptic mechanisms for two reasons. First, NE reduced the amplitude of the evoked EPSCs and IPSCs without changing their decay time constant, suggesting that the properties of postsynaptic glutamate and $GABA_A$ receptors were not affected by α_2-AR activation. Second, the reduction in synaptic transmission by NE persisted in the presence of barium, which blocks the small postsynaptic conductance change due to activation of the inwardly rectifying potassium current. Hence, most of the inhibition of the synaptic currents by NE is due to presynaptic mechanisms.

The effect of α_2-AR stimulation on synaptic transmission probably occurs in part via inhibition of voltage-dependent calcium channels that are located on the nerve terminals. However, our preliminary results indicate that additional mechanisms must be involved, because a decrease in the frequency of mEPSCs by NE could still be obtained in the presence of cadmium (200 μM), which blocks all known voltage-dependent calcium channels. One possible mechanism could be the inhibition of cAMP production via α_2-ARs (42).

Physiological implications. Recent gene substitution experiments (D79N α_2-AR mutant mouse) have suggested that α_{2A}-adrenoceptor activation mediates the hypotensive effect of imidazoline-related drugs (clonidine, moxonidine, rilmenidine) (24, 45). α_{2A}-Adrenoceptors are most likely responsible for the effects of NE observed in the present study, because the inhibitory actions of NE were obtained in the presence of prazosin (1 μM), which blocks α_1-adrenoceptors and antagonizes much of the effects of NE on α_{2B}- and α_{2C}-adrenoceptors (14). In addition, the presence of the α_{2A}-receptor subtype has been identified in the bulbospinal C1 cells (10).

The present study confirms that the postsynaptic inhibition of C1 and other bulbospinal RVLM neurons by α_2-AR agonists is variable, generally weak, and even lacking in some cells (18). This mechanism involves the opening of a barium-sensitive potassium current. In contrast, α_2-ARs cause a consistent and robust presynaptic inhibition of EPSCs. In combination, these two inhibitory mechanisms probably account for the bulk of the powerful sympathoinhibition produced by centrally acting antihypertensive agents in RVLM (8). However, NE does not produce purely inhibitory effects on bulbospinal RVLM neurons, because it also reduces the strength of at least some of the GABAergic inputs to these cells. This result is not totally unexpected because α_2-AR-mediated disinhibition of RVLM sympathoexcitatory presympathetic neurons was suggested by a recent in vivo study in which hypertension was produced by microinjection of clonidine into the caudal ventrolateral medulla, an area that provides tonic GABAergic inhibition to RVLM (36). Moreover, activation of other receptors like μ-opioid and $GABA_B$ receptors was also shown to attenuate both excitatory and inhibitory synaptic transmission in the RVLM (11, 21). Because α_2-AR agonists produce profound inhibition of

sympathetic outflow when microinjected in the RVLM (reviewed by Ref. 32), disfacilitation of RVLM presympathetic neurons by α_2-AR agonists must greatly outweigh disinhibition. This interpretation is consistent with the suggestion that most of the ongoing discharge of these neurons in vivo may result from fast excitatory postsynaptic potentials (26).

In conclusion, presynaptic α_2-ARs in the RVLM are probable targets of centrally acting antihypertensive drugs related to clonidine in addition to the previously described postsynaptic α_2-ARs (reviewed in Ref. 8). This conclusion is congruent with recent electron microscopic evidence that α_2-AR immunoreactivity in RVLM is found predominantly on noncatecholaminergic axons and axon terminals (26). The α_2-AR-mediated presynaptic inhibition of glutamate release would be especially effective in reducing the activity of the putative sympathoexcitatory neurons when their discharge derives from excitatory synaptic inputs rather than intrinsic membrane properties.

This work was supported by National Heart, Lung, and Blood Institute Grant HL-28785 (to P. G. Guyenet).

Address for reprint requests and other correspondence: P. Guyenet, Box 448 HSC, Dept. of Pharmacology, Univ. of Virginia, Charlottesville, VA 22908 (E-Mail: pgg@virginia.edu).

Received 10 February 1999; accepted in final form 13 April 1999.

REFERENCES

1. **Allen, A., M., and P. G. Guyenet.** α_2-Adrenoceptor-mediated inhibition of bulbospinal barosensitive cells of rat rostral medulla. *Am. J. Physiol.* 265 (*Regulatory Integrative Comp. Physiol.* 34): R1065–R1075, 1993.
2. **Bayliss, D. A., Y. W. Li, and E. M. Talley.** Effects of serotonin on caudal raphe neurons: inhibition of N- and P/Q-type calcium channels and the afterhyperpolarization. *J. Neurophysiol.* 77: 1362–1374, 1997.
3. **Bennett, B. D., J. R. Huguenard, and D. A. Prince.** Adrenergic modulation of $GABA_A$ receptor-mediated inhibition in rat sensorimotor cortex. *J. Neurophysiol.* 79: 937–946, 1998.
4. **Bertolino, M. S. Vicini, R. Gillis, and A. Travagli.** Presynaptic α_2-adrenoceptors inhibit excitatory synaptic transmission in rat brain stem. *Am. J. Physiol.* 272 (*Gastrointest. Liver Physiol.* 35): G654–G661, 1997.
5. **Chium, T. H., M. J. Chen, Y. R. Yang, J. J. Yang, and F. I. Tang.** Action of dexmedetomidine on rat locus coeruleus neurones: intracellular recording in vitro. *Eur. J. Pharmacol.* 285: 261–268, 1995.
6. **Deuchards, S. A., S. F. Morrison, and M. P. Gilbey.** Medullary-evoked EPSPs in neonatal rat sympathetic preganglionic neurones in vitro. *J. Physiol. (Lond.)* 487: 453–463, 1995.
7. **Doze, V. A., G. A. Cohen, and D. V. Madison.** Synaptic localization of adrenergic disinhibition in the rat hippocampus. *Neuron* 6: 889–900, 1991.
8. **Guyenet, P. G.** Is the hypotensive effect of clonidine and related drugs due to imidazoline binding sites? *Am. J. Physiol.* 273 (*Regulatory Integrative Comp. Physiol.* 42): R1580–R1584, 1997.
9. **Guyenet, P. G., N. Koshiya, D. Huangfu, S. C. Baraban, R. L. Stornetta, and Y. W. Li.** Role of medulla oblongata in generation of sympathetic and vagal outflows. *Prog. Brain Res.* 107: 127–144, 1996.
10. **Guyenet, P. G., R. L. Stornetta, T. Riley, F. R. Norton, D. L. Rosin, and K. R. Lynch.** α_{2A}-Adrenergic receptors are present in lower brainstem catecholaminergic and serotonergic neurons innervating spinal cord. *Brain Res.* 638: 285–294, 1994.
11. **Hayar, A., and P. Guyenet.** Pre- and postsynaptic inhibitory actions of methionine-enkephalin on identified bulbospinal neurons of the rat rostral ventrolateral medulla. *J. Neurophysiol.* 80: 2003–2014, 1998.
12. **Hayar, A., and P. Guyenet.** Presynaptic effects mediated by α_2-adrenoceptors (α_2-AR) in the rat rostral ventrolateral medulla (RVL) in vitro. *Soc. Neurosci. Abstr.* 24: 372, 1998.
13. **Hayar, A., P. Feltz, and P. Piguet.** Adrenergic responses in silent and putative inhibitory pacemaker-like neurons of the rat rostral ventrolateral medulla in vitro. *Neuroscience* 77: 199–217, 1997.
14. **Hieble, J. P., and R. R. Ruffolo, Jr.** Subclassification and nomenclature of α_1- and α_2-adrenoceptors. *Prog. Drug Res.* 47: 81–130, 1996.
15. **Huangfu, D., and P. G. Guyenet.** α_2-Adrenergic autoreceptors in A5 and A6 neurons of neonate rats. *Am. J. Physiol.* 273 (*Heart Circ. Physiol.* 42): H2290–H2295, 1997.
16. **Huangfu, D., M. Schreihofer, and P. G. Guyenet.** Effect of cholinergic agonists on bulbospinal C1 neurons in rats. *Am. J. Physiol.* 272 (*Regulatory Integrative Comp. Physiol.* 41): R249–R258, 1997.
17. **Kangrga, I. M., and A. D. Loewy.** Whole-cell recordings from visualized C1 adrenergic bulbospinal neurons: ionic mechanisms underlying vasomotor tone. *Brain Res.* 670: 215–232, 1995.
18. **Li, Y. W., D. A. Bayliss, and P. G. Guyenet.** C1 neurons of neonatal rats: intrinsic beating properties and α_2-adrenergic receptors. *Am. J. Physiol.* 269 (*Regulatory Integrative Comp. Physiol.* 38): R1356–R1369, 1995.
19. **Li, Y. W., and P. G. Guyenet.** Activation of $GABA_B$ receptors increases a potassium conductance in rat bulbospinal neurons of the C1 area. *Am. J. Physiol.* 271 (*Regulatory Integrative Comp. Physiol.* 40): R1304–R1310, 1996.
20. **Li, Y. W., P. G. Guyenet, and D. A. Bayliss.** Voltage-dependent calcium currents in bulbospinal neurons of neonatal rat rostral ventrolateral medulla: modulation by α_2-adrenergic receptors. *J. Neurophysiol.* 79: 583–594, 1998.
21. **Lin, H. H., and N. J. Dun.** Post- and presynaptic GABA(B) receptor activation in neonatal rat rostral ventrolateral medulla neurons in vitro. *Neuroscience* 86: 211–220, 1998.
22. **Lipski, J., R. Kanjhan, B. Kruszewska, and W. Rong.** Properties of presympathetic neurones in the rostral ventrolateral medulla in the rat: an intracellular study "in vivo." *J. Physiol. (Lond.)* 490: 729–744, 1996.
23. **Lipski, J., Y. Kawai, J. Qi, A. Comer, and J. Win.** Whole cell patch-clamp study of putative vasomotor neurons isolated from the rostral ventrolateral medulla. *Am. J. Physiol.* 274 (*Regulatory Integrative Comp. Physiol.* 43): R1099–R1110, 1998.
24. **MacMillan, L. B., L. Hein, M. S. Smith, M. T. Piascik, and L. E. Limbird.** Central hypotensive effects of the α_{2a}-adrenergic receptor subtype. *Science* 273: 801–803, 1996.
25. **Mienville, J. M., and S. Vicini.** A pyridazinyl derivative of gamma-aminobutyric acid (GABA), SR 95531, is a potent antagonist of Cl^- channel opening regulated by $GABA_A$ receptors. *Neuropharmacology* 26: 779–783, 1987.
26. **Milner, T. A., D. L. Rosin, A. Lee, and S. A. Aicher.** α_{2A}-Adrenergic receptors are primarily presynaptic heteroreceptors in the C1 area of the rat rostral ventrolateral medulla. *Brain Res.* 821: 200–211, 1999.
27. **Morrison, S. F., J. Callaway, T. A. Milner, and D. J. Reis.** Rostral ventrolateral medulla: a source of the glutamatergic innervation of the sympathetic intermediolateral nucleus. *Brain Res.* 562: 126–135, 1991.
28. **O'Rourke, M. F., H. S. Blaxall, L. J. Iversen, and D. B. Bylund.** Characterization of [^{3}H]RX821002 binding to α_2-adrenergic receptor subtypes. *J. Pharmacol. Exp. Ther.* 268: 1362–1367, 1994.
29. **Piguet, P., and R. Schlichter.** Lability of the pacemaker activity in the rat rostro-ventrolateral medulla: effects of noradrenaline. *Brain Res.* 796: 1–12, 1998.
30. **Prichard, B. N., C. W. Owens, and B. R. Graham.** Pharmacology and clinical use of moxonidine, a new centrally acting sympatholytic antihypertensive agent. *J. Hum. Hypertens.* 11: S29–S45, 1997.
31. **Punnen, S., R. Urbanski, A. J. Krieger, and H. N. Sapru.** Ventrolateral medullary pressor area: site of hypotensive action of clonidine. *Brain Res.* 422: 336–346, 1987.
32. **Reis, D. J.** Neurons and receptors in the rostroventrolateral medulla mediating the antihypertensive actions of drugs acting

at imidazoline receptors. *J. Cardiovasc. Pharmacol*. 27: S11–S18, 1996.

33. **Ross, C. A., D. A. Ruggiero, T. H. Joh, D. H. Park, and D. J. Reis.** Rostral ventrolateral medulla: selective projections to the thoracic autonomic cell column from the region containing C1 adrenaline neurons. *J. Comp. Neurol*. 228: 168–185, 1984.
34. **Ruggiero, D. A., S. L. Cravo, E. Golanov, R. Gomez, M. Anwar, and D. J. Reis.** Adrenergic and non-adrenergic spinal projections of a cardiovascular-active pressor area of medulla oblongata: quantitative topographic analysis. *Brain Res*. 663: 107–120, 1994.
35. **Sakmann, B., and G. Stuart.** Patch-pipette recordings from the soma, dendrites, and axon of neurons in brain slices. In: *Single-Channel Recording*, edited by B. Sakmann, and E. Neher. New York: Plenum, 1995, p. 199–211.
36. **Sesoko, S., H. Muratani, M. Yamazato, H. Teruya, S. Takishita, and K. Fukiyama.** Contribution of α_2-adrenoceptors in caudal ventrolateral medulla to cardiovascular regulation in rat. *Am. J. Physiol*. 274 (*Regulatory Integrative Comp. Physiol*. 43): R1119–R1124, 1998.
37. **Shen, K. Z., R. A. North, and A. Surprenant.** Potassium channels opened by noradrenaline and other transmitters in excised membrane patches of guinea-pig submucosal neurones. *J. Physiol. (Lond.)* 445: 581–599, 1992.
38. **Sun, M. K., and P. G. Guyenet.** Excitation of rostral medullary pacemaker neurons with putative sympathoexcitatory function by cyclic AMP and β-adrenoceptor agonists "in vitro." *Brain Res*. 511: 30–40, 1990.
39. **Travagli, R. A., and J. T. Williams.** Endogenous monoamines inhibit glutamate transmission in the spinal trigeminal nucleus of the guinea-pig. *J. Physiol. (Lond.)* 491: 177–185, 1996.
40. **Trombley, P. Q.** Noradrenergic modulation of synaptic transmission between olfactory bulb neurons in culture: implications to olfactory learning. *Brain Res. Bull*. 35: 473–484, 1994.
41. **Tucker, D. C., C. B. Saper, D. A. Ruggiero, and D. J. Reis.** Organization of central adrenergic pathways. I. Relationships of ventrolateral medullary projections to the hypothalamus and spinal cord. *J. Comp. Neurol*. 259: 591–603, 1987.
42. **Uhlen, S., and J. E. Wikberg.** Inhibition of cyclic AMP production by α_2-adrenoceptor stimulation in the guinea-pig spinal cord slices. *Pharmacol. Toxicol*. 63: 178–182, 1988.
43. **Vaughan, C. W., and M. J. Christie.** Presynaptic inhibitory action of opioids on synaptic transmission in the rat periaqueductal grey in vitro. *J. Physiol. (Lond.)* 498: 463–472, 1997.
44. **Zadina, J. E., L. Hackler, L. J. Ge, and A. J. Kastin.** A potent and selective endogenous agonist for the μ-opiate receptor. *Nature* 386: 499–502, 1997.
45. **Zhu, Q. -M., S. J. Maclennan, J. D. Lesnick, J. R. Jasper, R. M. Eglen, and D. R. Blue, Jr.** α_{2A}-Adrenoceptors, not I1-imidazoline receptors, mediate the hypotensive effects of rilmenidine and moxonidine: in vitro and in vivo studies (Abstract). *FASEB J*. 12: A455, 1998.